Liquid ^{3}He. I. Calculation of the Binding Energy from Two-Body Correlations*

E. ØSTGAARD
Palmer Physical Laboratory, Princeton University, Princeton, New Jersey 08540
(Received 4 January 1968)

As the first step in a theoretical study of the properties of liquid ^{3}He, we have calculated the binding energy of the system by means of Brueckner theory. The method of Brueckner and Gammel is used to solve the Bethe-Goldstone equation, calculate the reaction matrix or G matrix, and then get the two-body interaction energy contribution. The Brueckner-Gammel method is studied in some detail. For simplicity we use the approximation of an effective mass in a reference energy spectrum, which in principle should be fitted to self-consistent single-particle energies. The intermediate-state potential energies are, however, chosen to be equal to zero. Hence, the three-body energy contribution must be estimated by separate calculations. Various two-body wave functions, Fourier transforms of wave functions, and G-matrix elements are calculated. Also, the volume of the correlation hole, which gives the convergence parameter in the linked-cluster expansion, and an effective interaction, which is a representation of the G matrix in coordinate space, are calculated, together with the binding energy for liquid ^{3}He. The calculations are repeated for various input parameters, i.e., for several values of the parameters which define the reference energy spectrum, and for several values of the initial relative momentum of the two interacting particles. The total or c.m. momentum is set equal to zero. The Brueckner-Gammel method is found to be a fairly rapid and convenient method when the complete Green's function in the Bethe-Goldstone equation is expressed in terms of a corresponding reference-spectrum Green's function, and the single-particle energies in the energy denominator in the Bethe-Goldstone equation are replaced by a reference energy spectrum. Third-order and higher-order energy contributions can probably be assumed to be built into this energy spectrum, or they may be estimated by separate calculations. The binding energy for liquid ^{3}He with only two-body terms included is found to be approximately $-\frac{1}{2}$°K per particle, which is in general agreement with other calculations.

1. INTRODUCTION

THE simplest microscopic theory of liquid ^{3}He would be that of an ideal Fermi gas, but this obviously cannot be a good description of the real liquid ^{3}He. A pure Hartree-Fock theory is not useful either, because the interatomic potential is strongly repulsive at short distances, and two-body correlations must be included to get finite results. A hard-sphere gas has been studied in the low-density limit, but this work is of only formal interest to us, since liquid ^{3}He cannot be considered as a dilute system. The range of the forces is not small compared to the average spacing between the atoms, and we also need attraction to obtain binding of the system. We must, in principle, sum an infinite class of terms in the perturbation series to take into account the strong interactions between ^{3}He atoms. This can be done in a systematic way with diagrammatic perturbation theory.

The first serious attempt to calculate the properties of liquid ^{3}He at zero temperature from first principles was made by Brueckner and Gammel (BG).[1] The physical basis of the Brueckner theory is that when two ^{3}He atoms interact, they interact strongly, but at the same time the liquid is sufficiently dilute that their interaction with other particles may be considered in an average way. Brueckner and collaborators developed a method to avoid the difficulties resulting from the strong repulsion in the potential v. Starting from the linked Rayleigh-Schrödinger perturbation expansion for the energy, a rearrangement is performed which replaces the expansion in terms of the large matrix elements of the potential by an expansion in reaction matrix elements. This reaction matrix, or G matrix, is obtained by a solution of the two-body problem in the medium.

The multiple scattering theory of Brueckner is formalized by Goldstone[2] in the language of second quantization. The ground-state energy of the system is obtained as the sum of a perturbation series in the two-body interaction, where each term in the series is represented by a linked diagram. Linked diagrams are diagrams which cannot be separated into independent parts without breaking at least one interaction line. One hopes that the Goldstone series converges sufficiently rapidly for practical calculations, but this is not obvious because of the very strong short-range repulsion in the potential. However, the wave function is finite, and vanishes in this region. Then the G matrix corresponding to multiple elementary collisions is introduced, and the corresponding terms in the Goldstone expansion are the ladder diagrams, where a given pair of particles outside the Fermi sea interact any number of times with each other. The set of all such diagrams can be summed, and replaced by a single diagram in which the pair of particles interact by the G matrix.

Brueckner and Gammel calculate the interaction between two atoms, taking the rest of the medium into account in two important ways. The Pauli exclusion principle is included, which limits the number of states

* Work supported in part by the U. S. Atomic Energy Commission and the Higgins Scientific Trust Fund.

[1] K. A. Brueckner and J. L. Gammel, Phys. Rev. **109**, 1040 (1958).

[2] J. Goldstone, Proc. Roy. Soc. (London) **A239**, 267 (1957).

available for the interaction pair of atoms. Also, this pair of particles moves in an average field or self-consistent potential created by the neighbors. Effects from three-body or higher-order clusters are neglected. The motion of an atom is characterized by a momentum quantum number, and the ordering of states is like the ordering in a Fermi gas, but the atomic motion is associated with very strong polarization effects among the surrounding atoms, so the particles in the theory are really quasiparticles, or atoms moving with their polarization cloud. To include the exclusion principle and modified energy spectrum effects, BG use a Green's-function method to evaluate the G-matrix propagator in coordinate space. Their results are in reasonable agreement with experimental results, and may suggest that two-body correlations are the most important ones in describing liquid ^{3}He. But their calculated binding energy is less than half the experimental value.

In the integral equation for the G matrix, single-particle potentials expressed by diagonal elements of the G matrix are included. This introduces a problem of self-consistency. This single-particle energy spectrum is assumed to have a gap at the Fermi surface. Single-particle potentials representing the interaction with particles in the Fermi sea should be calculated on the energy shell. But when the medium is excited, scattering of a pair of particles occurs off the energy shell, and the single-particle potential for particles above the Fermi level should be calculated with G-matrix elements off the energy shell. In their nuclear-matter calculations, BG[3] approximate this by an average excitation of the order of magnitude of the Fermi energy, which is probably a rather bad approximation. Furthermore, they simply cut off the single-particle potential energy spectrum in intermediate states at the point where it goes through zero.[4] Although this gives results not too different from ours, it is inconsistent with their stated procedure, and it is clear that if they had retained the potential energy after it became positive, they would have obtained less binding energy. Perhaps the system would not have been bound at all. It is therefore important to redo their calculations in some consistent way.

The Brueckner method can be modified somewhat. For nuclear matter, Bethe *et al.*[5] have developed a method to calculate a relatively simple reference reaction matrix. The self-consistent single-particle spectrum is represented by a quadratic expression, i.e., an effective-mass approximation with appropriate coefficients. The release of the energy denominator from the loop of self-consistency through the G matrix and the single-particle energies is a great advantage and a major simplification in practical calculations. We will try to use this idea also in our calculations.

[3] K. A. Brueckner and J. L. Gammel, Phys. Rev. **109**, 1023 (1958).
[4] K. A. Brueckner (private communication).
[5] H. A. Bethe, B. H. Brandow, and A. G. Petschek, Phys. Rev. **129**, 225 (1963).

There remains some question about the single-particle energy spectrum for intermediate states. Bethe has proposed to calculate the three-body energy as if it were a self-energy correction to the two-body terms. One can define the particle potential energies in such a way that the three-body correlation energy is compensated by the potential insert diagrams of the Goldstone theory. The total energy is then given by the first-order two-body interactions, by summation of two-body terms. We will, however, in contrast to this method, choose the intermediate-state potentials to be zero, i.e., assume just free propagation or plane waves for the intermediate states, and then do separate calculations for the three-body cluster energy.

2. BRUECKNER-GAMMEL METHOD

In the method of BG,[1,3] the energy is calculated from a reaction matrix similar to the transition matrix for scattering in free space. This reaction matrix, or G matrix, is defined by the integral equation

$$G=v-v(Q/e)G \tag{2.1}$$

in operator form. Here v is the two-body potential, which is assumed to be the same as in free space. The Pauli exclusion operator Q prevents scattering into occupied intermediate states, i.e.,

$$\begin{aligned} Q(k_a,k_b)&=1 \text{ if } k_a>k_F \text{ and } k_b>k_F, \\ &=0 \text{ otherwise.} \end{aligned} \tag{2.2}$$

This is the exclusion-principle effect of the other particles in the medium on the two strongly interacting particles.

The energy operator e includes potential and kinetic energy, and can be written as

$$e=\epsilon_a+\epsilon_b-\epsilon_m-\epsilon_n. \tag{2.3}$$

The single-particle energies ϵ_m and ϵ_n are self-consistent energies for particles moving in the Fermi sea, and ϵ_a and ϵ_b are energies of virtual excitations above the Fermi surface.

The energy of an unexcited atom is

$$\epsilon(k_n)=T(k_n)+U(k_n), \tag{2.4}$$

where T is the kinetic energy,

$$T(k_n)=\tfrac{1}{2}\hbar^2k_n^2/M, \tag{2.5}$$

and M is the atomic mass.

It is a problem of particular importance and difficulty to define the single-particle energies ϵ. In the theory of Brueckner, the single-particle potential U is given by the diagonal elements of the G matrix by the relation

$$U(k_n)=\sum_m [\langle k_mk_n|G|k_mk_n\rangle-\langle k_mk_n|G|k_nk_m\rangle], \tag{2.6}$$

with summation over all occupied states. The second term in Eq. (2.6) comes from exchange of spin and mo-

mentum coordinates. If we assume that G is a function of only the magnitude of the total momentum P, we can write a partial-wave expansion

$$\langle k_m k_n|G|k_m k_n\rangle=\sum_L (2L+1)G_L(P,k_{mn})P_L(\cos\theta), \quad (2.7)$$

where G_L is a function of relative and c.m. momenta. The properties of the liquid can then be determined from the G matrix.

The total ground-state energy is

$$E=\sum_n [T(k_n)+\tfrac{1}{2}U(k_n)]. \quad (2.8)$$

We introduce relative and c.m. coordinates by defining

$$\begin{aligned}\mathbf{P}&=\tfrac{1}{2}(\mathbf{k}_1+\mathbf{k}_2),\\ \mathbf{k}&=\tfrac{1}{2}(\mathbf{k}_1-\mathbf{k}_2),\\ \mathbf{R}&=\tfrac{1}{2}(\mathbf{r}_1+\mathbf{r}_2),\\ \mathbf{r}&=\mathbf{r}_1-\mathbf{r}_2.\end{aligned} \quad (2.9)$$

Then $\mathbf{P}$ is the average momentum of the two particles, and the c.m. momentum is equal to $2\mathbf{P}$.

For central forces only, the angular-momentum reduction of the G matrix is given by

$$\langle \mathbf{k}'|G|\mathbf{k}\rangle=\sum_L (2L+1)\langle k'|G_L|k\rangle P_L(\hat{k}'\cdot\hat{k}). \quad (2.10)$$

Equation (2.4) for the energy of a particle moving on the energy shell with momentum k_n becomes

$$\begin{aligned}\epsilon(k_n)&=\tfrac{1}{2}\hbar^2 k_n^2/M\\ &+2\times 2\times\sum_m [\tfrac{1}{4}\sum_{\text{even } L}(2L+1)\langle k_{mn}|G_L|k_{mn}\rangle\\ &+\tfrac{3}{4}\sum_{\text{odd } L}(2L+1)\langle k_{mn}|G_L|k_{mn}\rangle], \quad (2.11)\end{aligned}$$

with the sum over m taken over the Fermi sea. The first factor of 2 in the interaction term comes from two spin states per momentum state, the second factor of 2 comes from the exchange term. The factors $\frac{1}{4}$ and $\frac{3}{4}$ give the weights of the singlet-even and triplet-odd states. We will later include all these factors in our definition of the G matrix.

We now have an effective interaction between the quasiparticles, given by the G matrix which is density-dependent. If we neglect the exclusion principle and the average field from the other atoms, we can write

$$\begin{aligned}\langle \mathbf{k}'|G|\mathbf{k}\rangle&=-(4\pi\hbar^2/Mk)\\ &\times\{\sum_{\text{even } L}(2L+1)\delta_L(k)P_L(\hat{k}'\cdot\hat{k})(1-P_\sigma)\\ &+\sum_{\text{odd } L}(2L+1)\delta_L(k)P_L(\hat{k}'\cdot\hat{k})(3+P_\sigma)\}, \quad (2.12)\end{aligned}$$

where P_σ is the spin-exchange operator, and $\delta_L(k)$ is the scattering phase shift for relative momentum $\mathbf{k}$. Equation (2.12) is probably a good approximation for $L>3$, but for lower values of L, the many-body effects are important and the exclusion principle must be included. The potential is strong in the important region and polarization effects occur.

If $\mathbf{k}_0$ is the initial- and $\mathbf{k}$ is the intermediate-state relative momentum of the two interacting atoms, then the Pauli operator (2.2) is

$$\begin{aligned}Q&=1 \quad \text{if} \quad |\mathbf{P}+\mathbf{k}|>k_F \quad \text{and} \quad |\mathbf{P}-\mathbf{k}|>k_F,\\ &=0 \quad \text{otherwise,}\end{aligned} \quad (2.13)$$

and the energy denominator (2.3) is

$$\begin{aligned}e(k,k_0,P)&=\epsilon(\mathbf{P}+\mathbf{k})+\epsilon(\mathbf{P}-\mathbf{k})-H(k_0,P)\\ &=(\hbar^2/M)(k^2-k_0^2)+[U(\mathbf{P}+\mathbf{k})+U(\mathbf{P}-\mathbf{k})\\ &\quad -U(\mathbf{P}+\mathbf{k}_0)-U(\mathbf{P}-\mathbf{k}_0)]. \quad (2.14)\end{aligned}$$

The exclusion operator Q is approximated by its average over angles of $\mathbf{P}$, i.e.,

$$\begin{aligned}Q(P,k)&=0 \quad \text{if} \quad k^2+P^2\leq k_F^2,\\ &=1 \quad \text{if} \quad k-P\geq k_F,\\ &=(P^2+k^2-k_F^2)/(2Pk) \quad \text{otherwise.}\end{aligned} \quad (2.15)$$

The single-particle potential (2.6) can be written as

$$\begin{aligned}U(k)&=\frac{8}{\pi^2}\int_0^{(k_F-k)/2} k'^2\langle k'|G|k'\rangle dk' \quad (\text{for } k<k_F)\\ &+\frac{4}{\pi^2}\int_{|k_F-k|/2}^{(k_F+k)/2}\left(1+\frac{k_F^2-k^2-4k'^2}{4kk'}\right)\\ &\times\langle k'|G|k'\rangle dk', \quad (2.16)\end{aligned}$$

or

$$\begin{aligned}U(k)&=\frac{8}{\pi^2}\int_0^{(k_F-k)/2} k'^2[\sum_{\text{even } L}+3\sum_{\text{odd } L}](2L+1)\\ &\times\langle k'|G_L|k'\rangle dk'+\frac{4}{\pi^2}\int_{|k_F-k|/2}^{(k_F+k)/2} k'^2\left(1+\frac{k_F^2-k^2-4k'^2}{4kk'}\right)\\ &\times[\sum_{\text{even } L}+3\sum_{\text{odd } L}](2L+1)\langle k'|G_L|k'\rangle dk'. \quad (2.17)\end{aligned}$$

For $k\geq k_F$ the first integral vanishes.

The average binding energy per particle is then

$$E_B=(3/k_F^3)\int_0^{k_F} k^2\left[\frac{\frac{1}{2}\hbar^2k^2}{M}+\tfrac{1}{2}U(k)\right]dk. \quad (2.18)$$

Further details of our calculations are given in Sec. 3. But first, for purposes of comparison, we will explain more about the original BG method.

The Fermi momentum, $p_F=\hbar k_F$, is related to the density by

$$p_F=\hbar(3\pi^2N/\Omega)^{1/3}, \quad (2.19)$$

where N is the total number of particles in a large volume Ω. The normal density can then be determined from the minimum of E_B, Eq. (2.18), as a function of

the density

$$\rho = N/\Omega = \tfrac{1}{3}k_F^3/\pi^2, \tag{2.20}$$

which gives the number of states in the Fermi sea.

The single-particle energies show a dispersive effect of the medium, which corresponds to a particle moving in an effective potential arising from its interaction with all other particles in the system. For hole states, these single-particle energies should be calculated on the energy shell, but for intermediate particle states they should be calculated off the energy shell. We then have an equation similar to Eq. (2.4) for the energy of an excited particle, but with a single-particle potential $U(k)$ calculated from excited-state G-matrix elements. In the BG calculations this is approximated by introducing into the energy denominator (2.3) a mean excitation energy or parameter Δ equal to the excitation energy of the Fermi gas. The virtual energies, defined in this way, then differ at the Fermi surface by an energy gap, which ensures nonsingular G-matrix elements. So, for propagation off the energy shell, BG replace Eq. (2.14) by

$$e(k,k_0,P) = \epsilon(k_+) + \epsilon(k_-) + \Delta - H(k_0,P), \tag{2.21}$$

where

$$k_\pm^2 = k^2 + P^2 \pm (2/\sqrt{3})PkQ^2(P,k). \tag{2.22}$$

They also replace the total momentum by a root-mean-square value of P, taken over pairs of particles in the Fermi sea, i.e.,

$$\langle P^2\rangle = \tfrac{3}{5}k_F(k_F - k_0)[1 + \tfrac{1}{3}k_0^2(2k_F^2 + k_0k_F)] \quad \text{for } k_0 \leq k_F, \tag{2.23}$$
$$= 0 \quad \text{otherwise.}$$

The quantitative agreement with experiments of the results of BG[1] for the binding energy is not quite satisfactory. They get a binding energy of -0.96°K per particle at a saturation distance of 2.60 Å. This equilibrium spacing is not so far from the experimental value of 2.43 Å,[6] but the binding energy is less than 40% of the experimental value of -2.5°K per particle.[7,8]

3. CALCULATION OF TWO-BODY TERMS

According to general scattering theory, the two-body wave function is defined by

$$G\Phi = v\Psi, \tag{3.1}$$

where Φ is the unperturbed free-particle wave function and Ψ is the perturbed one. The distortion of the wave function due to the potential is written as

$$\zeta = \Phi - \Psi. \tag{3.2}$$

Due to the strongly repulsive core, the momentum space matrix elements of the potential v are very large. The reaction matrix equation (2.1) is then reformulated and converted into coordinate space by defining a wave operator Ω, which replaces the uncorrelated wave function Φ by the correlated wave function Ψ, i.e.,

$$\Psi = \Omega\Phi. \tag{3.3}$$

Equation (3.1) is equivalent to the operator equation

$$G = v\Omega, \tag{3.4}$$

and its matrix element is

$$\langle\Phi|G|\Phi\rangle = \langle\Phi|v|\Psi\rangle. \tag{3.5}$$

Dividing Eq. (2.1) on the left by v and multiplying from the right by Φ, we get the Bethe-Goldstone equation[9]

$$\Psi = \Phi - (Q/e)v\Psi, \tag{3.6}$$

and for the wave operator

$$\Omega = 1 - (Q/e)G. \tag{3.7}$$

The propagator Q/e is a rather complicated nonlocal integral operator.

Equation (3.6) is written in coordinate space as

$$\Psi(\mathbf{r}) = \Phi(\mathbf{r}) + \int \Gamma(\mathbf{r},\mathbf{r}')v(\mathbf{r}')\Psi(\mathbf{r}')d^3r', \tag{3.8}$$

where the radial Green's function $\Gamma(\mathbf{r},\mathbf{r}')$ is

$$\Gamma(\mathbf{r},\mathbf{r}') = -(2\pi)^{-3}\int d^3k \frac{\exp i\mathbf{k}(\mathbf{r}-\mathbf{r}')}{e(k)}, \tag{3.9}$$

and $e(k)$ is the energy denominator (2.3).

The Bethe-Goldstone equation (3.8) is separated into partial waves by introducing the expansion

$$\Phi(\mathbf{r}) = \sum_L (2L+1)i^L j_L(k_0r)P_L(\hat{k}_0\cdot\hat{r})$$
$$= \sum_L (2L+1)i^L P_L(\cos\theta)\frac{\mathcal{J}_L(k_0r)}{(k_0r)}. \tag{3.10}$$

Then $\mathcal{J}_L(k_0r)$ corresponds to the free-particle wave function.

Expanding and defining in the same way the radial components χ_L of ζ and u_L of Ψ, we get

$$\begin{aligned} \mathcal{J}_L(k_0r) &= k_0r\cdot j_L(k_0r), \\ u_L(k_0,r) &= k_0r\cdot\Psi_L(k_0,r), \\ \chi_L(k_0,r) &= \mathcal{J}_L(k_0r) - u_L(k_0,r). \end{aligned} \tag{3.11}$$

We also define a partial-wave effective interaction or potential

$$g_L(r) = v(r)u_L(k_0,r)/\mathcal{J}_L(k_0r)$$
$$= v(r)[1 - \chi_L(k_0,r)/\mathcal{J}_L(k_0r)], \tag{3.12}$$

[6] E. C. Kerr, Phys. Rev. **96**, 551 (1954).
[7] S. G. Sydoriak and T. R. Roberts, Phys. Rev. **106**, 175 (1957).
[8] T. R. Roberts, R. H. Sherman, and S. G. Sydoriak, J. Res. Natl. Bur. Std. (U. S.) **68A**, 567 (1964).
[9] H. A. Bethe and J. Goldstone, Proc. Roy. Soc. (London) **A238**, 551 (1957).

so that

$$\int_0^\infty \mathcal{J}_L(k_0r)v(r)u_L(k_0,r)dr=\int_0^\infty \mathcal{J}_L^2(k_0r)g_L(r)dr. \quad (3.13)$$

In the reference-spectrum method of Bethe *et al.*[5] for nuclear matter, the G-matrix equation is solved with two important approximations. The basic idea is to approximate the operator Q/e by a simpler one. Then the equation can be solved analytically and the error in the approximation can be calculated by a perturbation method.

One approximation is to assume the energy denominator $e(k)$ to be a quadratic function of the relative momentum. We have also used this idea in our BG method in order to make calculations simpler.

Assuming a single-particle potential of the form

$$U(k)=A+Bk^2, \quad (3.14)$$

we can write for the energy of intermediate states

$$\begin{aligned}\epsilon(k)&=T(k)+U(k)\\&=A+Bk^2+T(k)=A+T(k)/m^*,\end{aligned} \quad (3.15)$$

where the constants A and m^* should be chosen to give a good approximation to the actual self-consistent energy in the important range for k. The constant A is probably rather close to zero, and m^* is the dimensionless effective mass. The constant B is

$$B=T(k)(1/m^*-1)/k^2=\tfrac{1}{2}(\hbar^2/M)(1/m^*-1). \quad (3.16)$$

The quadratic form (3.15) is equivalent to the differential operator

$$\epsilon(k)=A+\tfrac{1}{2}\hbar^2k^2/(Mm^*)=A-\tfrac{1}{2}(\hbar^2/Mm^*)\nabla^2. \quad (3.17)$$

For states in the Fermi sea, we can define an equation similar to Eq. (3.14) with A_0 instead of A, and the effective mass m_0^* for the hole spectrum of particles in the Fermi sea.

The energy denominator for two particles of relative momentum $\mathbf{k}$ and total momentum $2\mathbf{P}$, i.e., Eq. (2.14), is then

$$\begin{aligned}e(k)&=\epsilon(\mathbf{P}+\mathbf{k})+\epsilon(\mathbf{P}-\mathbf{k})-H(k_0,P)\\&=-(\hbar^2/M)(\nabla^2-\gamma^2)/m^*\\&=(\hbar^2/M)(k^2+\gamma^2)/m^*,\end{aligned} \quad (3.18)$$

where

$$\gamma^2=2\Delta k_F^2-k_0^2m^*/m_0^* \quad (3.19)$$

for propagation on the energy shell and $k_0<k_F$. We see that γ^2 is a positive constant depending on the total momentum of the pair and on the starting energy. Δ is a measure of the gap between the occupied and the intermediate-state energy spectra. Then

$$\Delta=(Mm^*/\hbar^2k_F^2)(A-A_0), \quad (3.20)$$

and m^* and Δ are the basic parameters of the energy spectrum. We will later put $A=0$ and $m^*=1$. Then the gap Δ (or the parameter γ^2) just defines the hole spectrum, which will be our real input parameter.

One should determine the important range of intermediate-state energies by examining the statistical average of the square of the Fourier-Bessel transform of the distortion ζ in the wave function, or rather the partial-defect wave function χ_L/k_0. We are therefore interested in

$$F_L(k)=k_0^{-1}\int_0^\infty \mathcal{J}_L(kr)\chi_L(k_0,r)dr. \quad (3.21)$$

The Fourier transforms can be calculated in two different ways. One is to integrate Eq. (3.21) directly numerically, but this method is probably not the best one. From Eqs. (3.6) and (3.11) we see that we can write

$$\chi_L=\mathcal{J}_L-u_L=(Q/e)vu_L, \quad (3.22)$$

where the Pauli operator Q is defined by Eq. (2.15), i.e.,

$$\begin{aligned}Q(P,k)&=0 \quad \text{for} \quad k<\sqrt{(k_F^2-P^2)},\\&=(P^2+k^2-k_F^2)/(2Pk)\\&\qquad \text{for} \quad \sqrt{(k_F^2-P^2)}<k<k_F+P,\\&=1 \quad \text{for} \quad k>k_F+P,\end{aligned} \quad (3.23)$$

and the energy denominator e is defined by Eq. (3.18). Then the Fourier transforms are given by

$$F_L(k)=\frac{Q(P,k)m^*}{\gamma^2+k^2}k_0^{-1}\int_0^\infty \mathcal{J}_L(kr)v(r)u_L(k_0,r)dr. \quad (3.24)$$

Equation (3.24) is probably more accurate than Eq. (3.21), at least for $k\approx k_F$, and we have used the first one in our calculations. We see that the exclusion operator $Q(P,k)$ ensures correct behavior near k_F.

The volume integral

$$\kappa=\rho\int|\zeta(k_0,r)|^2d\tau=4\pi\rho\int_0^\infty|\zeta(k_0,r)|^2r^2dr, \quad (3.25)$$

or

$$\begin{aligned}\kappa&=4\pi\rho[\tfrac{1}{4}\sum_{\text{even }L}+\tfrac{3}{4}\sum_{\text{odd }L}](2L+1)\int_0^\infty\left(\frac{\chi_L}{k_0}\right)^2dr\\&=\pi\rho[\sum_{\text{even }L}+3\sum_{\text{odd }L}](2L+1)\\&\qquad\times\int_0^\infty\left(\frac{\chi_L}{k_0}\right)^2dr=\pi\rho\sum_L\kappa_L,\end{aligned} \quad (3.26)$$

is a very important quantity for the saturation properties of the system. It is proportional to the probability of finding a particle in an excited state rather than in the Fermi sea, and it is the hopefully small parameter which possibly characterizes the convergence of the rearranged linked-cluster expansion. In nuclear matter κ is of the order of 10–20%, but unfortunately it is rather large for liquid ^{3}He, as we shall see below. The

integral κ/ρ in Eq. (3.25) has been called the volume of the correlation hole, or the size of the wound in the wave function.

This volume integral of the square of the defect wave function $\chi(k_0,r)$, i.e., the integral in the expression (3.26) for κ, can be written as

$$\int_0^\infty \left(\frac{\chi_L}{k_0}\right)^2 dr=\frac{2}{\pi}\int_{kF}^\infty F_L{}^2(k)dk \propto \kappa_L \propto \frac{\kappa}{\rho} \quad (3.27)$$

in dimension [Å^3], where $F_L(k)$ is the Fourier transform (3.24). We see that this integral can be calculated in two different ways, integrating $\chi_L(k_0,r)$ in coordinate space or $F_L(k)$ in momentum space. Because the integral is density-dependent and hence also κ_L defined by Eq. (3.26), we also calculate the density-independent expression for κ. To get κ as defined in Eq. (3.26) we then should multiply the results (3.27) by $4\pi\rho$ and include appropriate statistical factors for the different partial waves.

Potentials and energies can be expressed in units of °K=ergs/k, where k is Boltzmann's constant. But in the following sections we express energies in units of Å^{-2}, the conversion factor being

$$\hbar^2/M=16.36°\text{K Å}^2. \quad (3.28)$$

Also, to make the notation as simple as possible, indices are suppressed throughout the paper when they are not really necessary. All the wave functions are functions of the relative momentum k_0, unless otherwise stated.

The principal equations to be solved are the following:

After an angular-momentum reduction of Eq. (3.5), the diagonal G-matrix elements for the angular momentum L and relative momentum k_0 can be written as

$$\langle k_0|G_L|k_0\rangle \propto 4\pi\int r^2 j_L(k_0r)v(r)u_L(k_0,r)dr, \quad (3.29)$$

which we obtain from Eqs. (2.10) and (3.5). The free-scattering result, which we have used as an approximation for $L>3$, can be written as in Eq. (2.12), i.e.,

$$\langle k_0|G_L|k_0\rangle \propto -(4\pi/k_0)\delta_L(k_0). \quad (3.30)$$

Equations (3.5) and (3.29) are rewritten as

$$\langle k_0|G_0|k_0\rangle=\sum_L \langle k_0|G_L|k_0\rangle$$
$$=(4\pi/k_0{}^2)[\sum_{\text{even } L}+3\sum_{\text{odd } L}](2L+1)$$
$$\times\int_0^\infty \mathcal{J}_L(k_0r)v(r)u_L(k_0,r)dr, \quad (3.31)$$

and we take this as our definition of G_L, i.e., we include appropriate statistical factors.

For nondiagonal G-matrix elements, Eq. (3.31) is changed to

$$\langle k|G|k_0\rangle=\sum_L \langle k|G_L|k_0\rangle$$
$$=(4\pi/kk_0)[\sum_{\text{even } L}+3\sum_{\text{odd } L}](2L+1)$$
$$\times\int_0^\infty \mathcal{J}_L(kr)v(r)u_L(k_0,r)dr. \quad (3.32)$$

The single-particle energies (2.4) or (2.11) are given by

$$\epsilon(k)=\tfrac{1}{2}k^2/M+U(k), \quad (3.33)$$

where $U(k)$ is defined by Eq. (2.17). The binding energy can then be calculated according to Eq. (2.18).

The radial wave functions are given by the Bethe-Goldstone integral equation (3.8) in the form

$$u_L(k_0,r)=\mathcal{J}_L(k_0r)+\int_0^\infty \Gamma_L(r,r')v(r')u_L(k_0,r')dr'. \quad (3.34)$$

The Green's functions $\Gamma_L(r,r')$ are defined by

$$\Gamma_L(r,r')=-\frac{2}{\pi}\int_0^\infty dk\frac{\mathcal{J}_L(kr)\mathcal{J}_L(kr')Q(P,k)m^*}{\gamma^2+k^2} \quad (3.35)$$

for propagation off the energy shell in the intermediate states, where $Q(P,k)$ is given by Eq. (3.23).

All the integrals have been calculated by numerical integration and performed by means of Simpson's rule or with a trapezoidal method.

The Green's functions $\Gamma_L(r,r')$ are computed first. This is a time-consuming part of the calculations and the release of the energy denominator from the requirement of self-consistency is a great simplification here. For each partial wave u_L, the continuum $0<r<\infty$ is replaced by a discrete set of points within the important range of the potential v. The corresponding radial Green's functions are evaluated for all pairs of points, and u_L is obtained by diagonalizing a finite matrix, i.e., by matrix inversion.

To obtain the integral (3.35) as accurately as possible, using the property of the Pauli step function (3.23), we write Eq. (3.35) in the form

$$\Gamma_L(r,r')=-\frac{2}{\pi}m^*\int_0^\infty dk\frac{\mathcal{J}_L(kr)\mathcal{J}_L(kr')}{\gamma^2+k^2}+\frac{2}{\pi}m^*$$
$$\times\int_0^{(k_F+P)} dk\frac{\mathcal{J}_L(kr)\mathcal{J}_L(kr')[1-Q(P,k)]}{\gamma^2+k^2}. \quad (3.36)$$

The first integral corresponds to a Green's function in which the exclusion principle is not included. For this $\Gamma_L{}^{(0)}(r,r')$ an analytic expression can be obtained.

Using Eq. (3.23), Eq. (3.36) is written

$$\Gamma_L(r,r')=\Gamma_L^{(0)}(r,r') +\frac{2}{\pi}m^*\int_0^{\sqrt{(k_F^2-P^2)}}dk\frac{\mathcal{J}_L(kr)\mathcal{J}_L(kr')}{\gamma^2+k^2}+\frac{2}{\pi}m^* \times\int_{\sqrt{(k_F^2-P^2)}}^{(k_F+P)}dk\frac{\mathcal{J}_L(kr)\mathcal{J}_L(kr')[k_F^2-(k-P)^2]}{2kP(\gamma^2+k^2)}, \quad (3.37)$$

where

$$\Gamma_L^{(0)}(r,r')=-\frac{2}{\pi}m^*\int_0^\infty dk\frac{\mathcal{J}_L(kr)\mathcal{J}_L(kr')}{\gamma^2+k^2}, \quad (3.38)$$

with the solution

$$\Gamma_L^{(0)}(r,r')=(m^*/2\gamma)[(-1)^L H_L^{(-)}(\gamma r)H_L^{(-)}(\gamma r') -H_L^{(-)}(\gamma r_>)H_L^{(+)}(\gamma r_<')] \quad (\text{for } r>r'). \quad (3.39)$$

Here

$$H_L^{(\pm)}(x)=i^{(L+1)}(\mp ix)h_L^{(1)}(\mp ix) =i^{-(L+1)}(\pm ix)h_L^{(2)}(\pm ix) \quad (3.40)$$

are the solutions $H_L(\gamma r)$ of the equation

$$[d^2/dr^2-L(L+1)/r^2-\gamma^2]H_L(\gamma r)=0, \quad (3.41)$$

expressed in terms of spherical Hankel functions. The latter are defined by

$$h_L^{(1)}=-ih_L^{(+)}, \quad h_L^{(2)}=ih_L^{(-)}, \quad (3.42)$$

where

$$h_L^{(\pm)}=n_L\pm ij_L. \quad (3.43)$$

For the lowest partial waves we get for Eq. (3.39) the solutions

$$\begin{aligned}
\Gamma_0^{(0)}(r,r')&=(m^*/2\gamma)\{\exp[-\gamma(r+r')]-\exp[-\gamma|r-r'|]\},\\
\Gamma_1^{(0)}(r,r')&=-(m^*/2\gamma)\{[1+1/\gamma r][1+1/\gamma r']\exp[-\gamma(r+r')]+[1\pm 1/\gamma r][1\mp 1/\gamma r']\exp[-\gamma|r-r'|]\},\\
\Gamma_2^{(0)}(r,r')&=(m^*/2\gamma)\{[1+3/\gamma r+3/(\gamma r)^2][1+3/\gamma r'+3/(\gamma r')^2]\exp[-\gamma(r+r')]\\
&\quad -[1\pm 3/\gamma r+3/(\gamma r)^2][1\mp 3/\gamma r'+3/(\gamma r')^2]\exp[-\gamma|r-r'|]\}, \quad (3.44)\\
\Gamma_3^{(0)}(r,r')&=-(m^*/2\gamma)\{[1+6/\gamma r+15/(\gamma r)^2+15/(\gamma r)^3][1+6/\gamma r'+15/(\gamma r')^2+15/(\gamma r')^3]\exp[-\gamma(r+r')]\\
&\quad +[1\pm 6/\gamma r+15/(\gamma r)^2\pm 15/(\gamma r)^3][1\mp 6/\gamma r'+15/(\gamma r')^2\mp 15/(\gamma r')^3]\exp[-\gamma|r-r'|]\},
\end{aligned}$$

and so on. In the expressions above, the upper sign is for $r>r'$, the lower sign is for $r<r'$.

The second integral in Eq. (3.36) can be calculated numerically with high precision. Some typical Green's functions are shown in Fig. 1.

The wave functions $u_L(r)$ are determined by numerical integration of Eq. (3.34). Because of the strongly repulsive part of the potential, we had great problems with an iteration procedure. It would not converge, and we had to use a matrix inversion directly to get the wave functions. Afterwards, the G-matrix elements are calculated by numerical integration.

4. PARAMETERS AND RESULTS

At zero pressure, near zero temperature, an atom occupies a mean volume define by

$$1/\rho=\Omega/N=\tfrac{4}{3}\pi r_0^3. \quad (4.1)$$

At normal mass density, which for liquid ^{3}He is 0.082 g/cm^3, the mean interparticle spacing r_0 is determined experimentally to be 2.43 Å.[6] At this density, the binding energy or mean energy at zero temperature is usually taken to be -5.04 cal/mole, or -2.53°K/particle.[7] The most recent value is, however, -4.92 cal/mole, or -2.47°K/particle,[8] so we take the experimental value to be just -2.5°K/particle. The Fermi momentum is given by Eqs. (2.20) and (4.1) as

$$k_F=(9/4\pi)^{1/3}/r_0=1.92/r_0=0.79 \text{ Å}^{-1}. \quad (4.2)$$

The average kinetic energy per particle of the Fermi gas is then

$$T_F=\tfrac{3}{10}\hbar^2k_F^2/M=18/r_0^2=3.05\text{°K}, \quad (4.3)$$

where M is the mass of the ^{3}He atom.

Brueckner and Gammel[1] have considered two potentials in their calculations. The first one is a Lennard-Jones[10] 6–12 potential of the form

$$V_{BM}(r)=V_0[(R/r)^{12}-(R/r)^6], \quad (4.4)$$

where

$$V_0=40.88\text{°K}, \quad R=2.56 \text{ Å}, \quad (4.5)$$

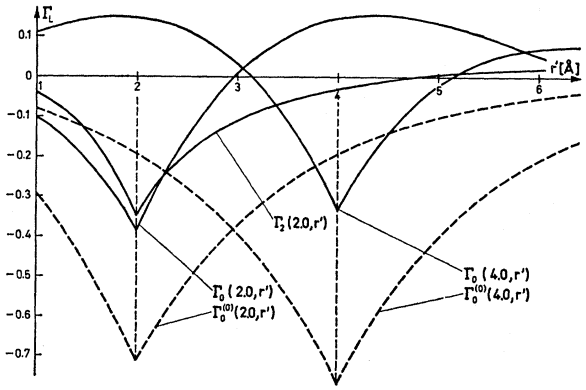

FIG. 1. Green's functions $\Gamma_L(r,r')$ for $L=0$ (and $L=2$). $\Gamma_0^{(0)}(r,r')$ (dotted line) is with the exclusion principle neglected, i.e., Eq. (3.44). $k_F=0.75$ Å^{-1}, $\Delta=0.5$, $m^*=1.0$, and $k_0=0.5k_F$.

[10] J. E. Lennard-Jones, Proc. Roy. Soc. (London) **A106**, 463 (1924).

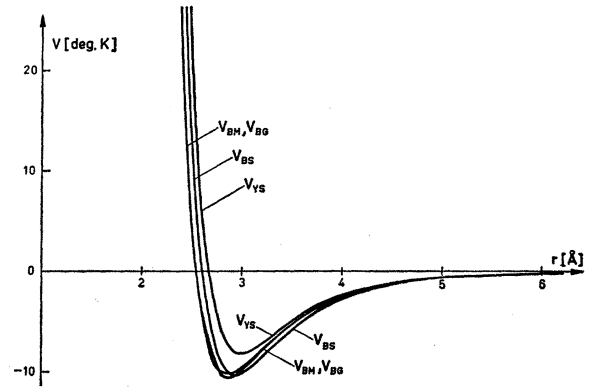

FIG. 2. Potentials for liquid ^{3}He. V_{BM} is given by Eq. (4.4), V_{BG} by Eq. (4.6), V_{BS} by Eq. (4.11), and V_{YS} by Eq. (4.13).

and r is measured in Å. This is a semiphenomenological potential fitted by de Boer and Michels[11] (BM) to the low-temperature virial coefficients.

The second potential is of the general form determined theoretically by Slater and Kirkwood[12] with an exponential repulsive term, but with parameters first calculated by Yntema and Schneider (YS),[13] fitted to the virial coefficients up to 1200°K. The Yntema-Schneider potential used by BG[1] is defined as

$$V_{BG}(r)=V_0[1200\exp(-4.82r) -1.24/r^6-1.89/r^8], \quad (4.6)$$

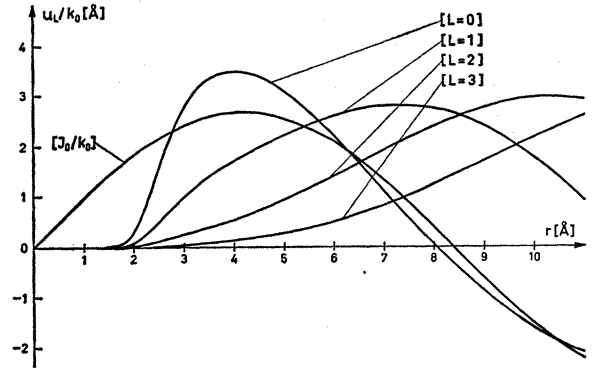

FIG. 3. Wave functions $\mathcal{J}_0(k_0r)$ and $u_L(k_0,r)$. $k_F=0.75$ Å^{-1}, $\Delta=0.5$, $m_0^*=1.5$, and $k_0=0.5k_F$.

where

$$V_0=7250°\text{K}, \quad (4.7)$$

and r is measured in Å.

The YS exp-6-8 potential can generally be written in the form[14]

$$V(r)=U_0\{g_1(\alpha,\beta)\exp[\alpha(1-r/R)] -g_2(\alpha,\beta)(R/r)^6[1+\beta(R/r)^2]\}, \quad (4.8)$$

where

$$g_1(\alpha,\beta)=(6+8\beta)/[\alpha(1+\beta)-(6+8\beta)],$$
$$g_2(\alpha,\beta)=\alpha/[\alpha(1+\beta)-(6+8\beta)]. \quad (4.9)$$

For the parameters in this potential, Buckingham and Scriven[15] (BS) have given the values

$$U_0=10.18°\text{K}, \quad R=2.943\text{ Å}, \quad \alpha=13.5, \quad \beta=0.20, \quad (4.10)$$

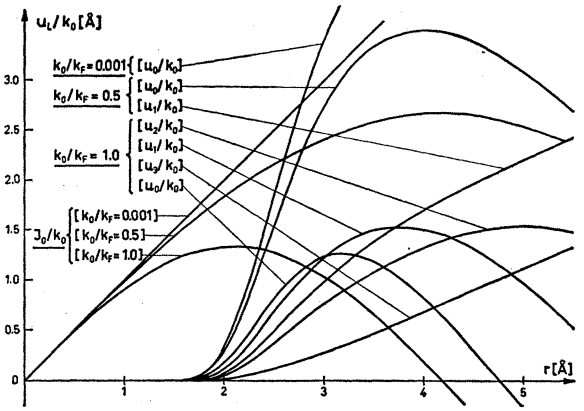

FIG. 4. Wave functions $\mathcal{J}_0(k_0r)$ and $u_L(k_0r)$. k_0 is varied. $k_F=0.75$ Å^{-1}, $\Delta=0.4$, and $m_0^*=2.0$.

which gives a potential written in the form (4.6) as

$$V_{BS}(r)=V_0[905\exp(-4.59r)-1.43/r^6-2.48/r^8]. \quad (4.11)$$

The corresponding data for the original YS potential are, according to de Boer,[14]

$$U_0=8.12°\text{K}, \quad R=3.0\text{ Å}, \quad \alpha=14.2, \quad \beta=0.17, \quad (4.12)$$

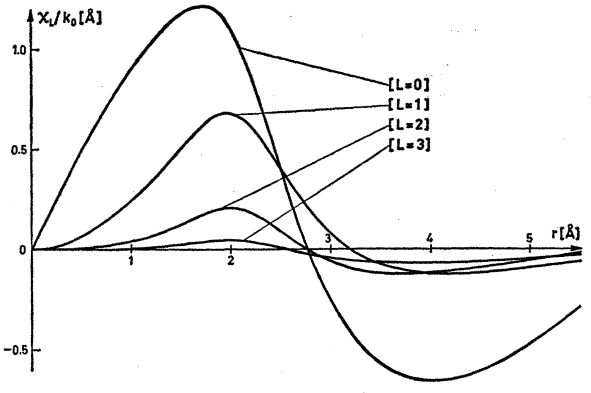

FIG. 5. Wave functions $\chi_L(k_0,r)$. $k_F=0.78$ Å^{-1}, $\Delta=0.4$, $m_0^*=2.0$, and $k_0=k_F$.

[11] J. de Boer and A. Michels, Physica **5**, 945 (1938).
[12] J. C. Slater and J. G. Kirkwood, Phys. Rev. **37**, 682 (1931).
[13] J. L. Yntema and W. G. Schneider, J. Chem. Phys. **18**, 646 (1950).
[14] J. de Boer, Physica Suppl. **24**, 90 (1958).
[15] R. A. Buckingham and R. A. Scriven, Proc. Phys. Soc. (London) **A65**, 376 (1952).

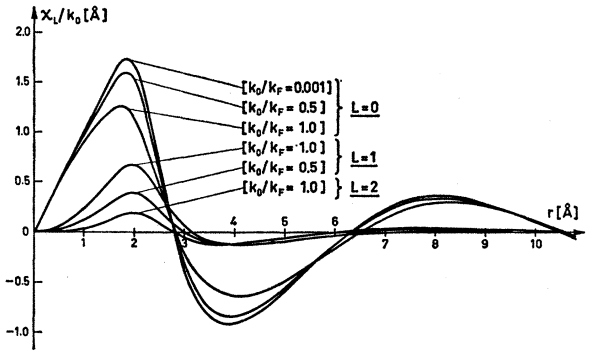

FIG. 6. Wave functions $\chi_L(k_0,r)$. k_0 is varied. $k_F=0.75$ Å^{-1}, $\Delta=0.4$, and $m_0^*=2.5$.

which gives a potential of the form (4.6) as

$$V_{YS}(r)=V_0[1308\exp(-4.73r) -1.25/r^6-1.91/r^8], \quad (4.13)$$

with V_0 given by Eq. (4.7). This is slightly different from the potential given by YS,[13] which is

$$V_{YS}(r)=V_0[1200\exp(-4.72r) -1.24/r^6-1.89/r^8], \quad (4.14)$$

but probably because the parameters (4.12) are derived from Eq. (4.14) and not vice versa. It is not obvious

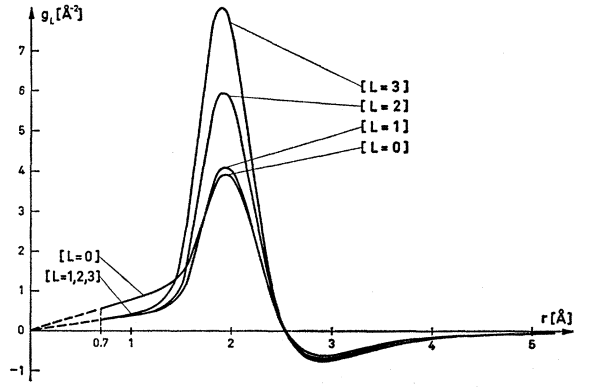

FIG. 7. Effective interactions $g_L(r)=v(r)u_L(k_0,r)/\mathcal{J}_L(k_0r)$. Calculated on the energy shell for $r>0.7$ Å. $k_F=0.78$ Å^{-1}, $\Delta=0.4$, $m_0^*=2.5$, and $k_0=0.5k_F$.

why BG have used the potential (4.6) rather than the potential (4.13) or (4.14) in their final calculations. But for comparison we have also used exactly the same potential (4.6) in all our calculations. The four potentials (4.4), (4.6), (4.11), and (4.13) are shown in Fig. 2.

The other parameters which we have used in the calculations are chosen in the following way:

Because BG got their self-consistent solution for

$$r_0=2.60 \text{ Å}, \quad k_F=0.74 \text{ Å}^{-1}, \quad (4.15)$$

while the experimental value is

$$r_0=2.43 \text{ Å}, \quad k_F=0.79 \text{ Å}^{-1}, \quad (4.16)$$

we have chosen two values for the Fermi momentum in our calculations, i.e.,

$$k_F=0.75 \text{ Å}^{-1} \text{ or } =0.78 \text{ Å}^{-1}. \quad (4.17)$$

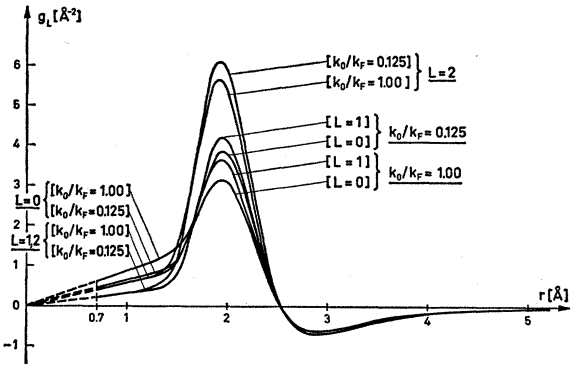

FIG. 8. Effective interactions $g_L(r)$. Calculated on the energy shell for $r>0.7$ Å. k_0 is varied. $k_F=0.75$ Å^{-1}, $\Delta=0.4$, and $m_0^*=2.0$.

The corresponding density is

$$\rho=\tfrac{1}{3}k_F^3/\pi^2=0.0142 \text{ Å}^{-3} \text{ or } =0.0160 \text{ Å}^{-3}. \quad (4.18)$$

and the corresponding average kinetic energy is

$$T_F=\tfrac{3}{10}\hbar^2k_F^2/M=2.76°\text{K} \text{ or } =2.99°\text{K}. \quad (4.19)$$

For the effective mass which defines the energy spectrum, we have also used different values. One reasonable approximation for the single-particle energy

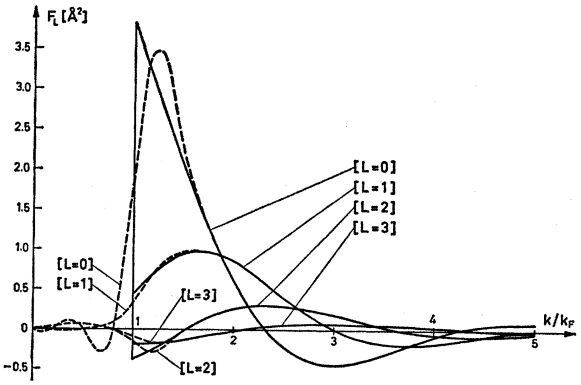

FIG. 9. Fourier transforms $F_L(k)$ of $\chi_L(k_0,r)/k_0$, defined by Eq. (3.24). Dotted lines indicate $F_L(k)$ calculated according to Eq. (3.21). $k_F=0.78$ Å^{-1}, $\Delta=0.4$, $m_0^*=2.0$, and $k_0=k_F$.

TABLE I. Diagonal G_0-matrix elements (in Å), calculated on the energy shell. RS method is with the exclusion principle neglected and Eq. (3.38) instead of Eq. (3.36) for the Green's functions $\Gamma_0(r,r')$. $L=0$, Δ is varied. $k_F=0.75$ Å^{-1}, $m_0^*=2.0$, and $k_0=0.5k_F$.

Δ	RS method	BG method
0.3	20.3	37.8
0.4	25.1	44.1
0.5	29.8	50.2

spectrum would be

$$\epsilon(k)=\tfrac{1}{2}k^2/m^*-\tfrac{1}{2}k_F^2/m^*+\mu \quad \text{for} \quad k\leq k_F, \qquad =\tfrac{1}{2}k^2 \quad \text{for} \quad k\geq k_F, \tag{4.20}$$

where μ is the chemical potential or separation energy:

$$\mu=E(N+1)-E(N) =(\partial E/\partial N)_\Omega=E/N+(\rho/N)(\partial E/\partial\rho), \tag{4.21}$$

TABLE II. Diagonal G_L-matrix elements (in Å), calculated on the energy shell, and V_L-matrix elements (in Å), defined by Eq. (4.30). Statistical weights included. k_0 is varied. $k_F=0.75$ Å^{-1}, $\Delta=0.4$, and $m_0^*=2.0$.

	$L=4$		$L=5$		$L=6$	
k_0/k_F	G_4	V_4	G_5	V_5	G_6	V_6
0.50	−0.42	−0.69	−0.21	−0.78	−0.01	−0.10
0.75	−2.33	−2.35	−2.46	−2.86	−0.26	−0.45
1.00	−5.58	−5.50	−6.84	−6.88	−1.07	−1.10

and the experimental value for μ is -2.5°K.[7,8] The energy spectrum (4.20) corresponds to free propagation of quasiparticles for large excitations. Therefore, if $m^*\approx 1$ off the energy shell, we may approximately replace the potential energy for particle states by a constant:

$$U(k)=\text{const}\approx 0 \quad \text{for} \quad k>k_F. \tag{4.22}$$

TABLE III. Diagonal G_L-matrix elements (in Å), calculated on the energy shell. Statistical weights included. k_0 is varied. $\Delta=0.4$ and $m_0^*=2.5$.

k_F(Å^{-1})	k_0/k_F	$L=0$	$L=1$	$L=2$	$L=3$	$L>3$	Total
0.75	0.001	5.1	0	0	0	0	5.1
	0.125	9.5	−12.3	−0.1	0	0	−2.9
	0.25	20.6	−39.4	−1.3	−0.3	0	−20.4
	0.375	33.6	−63.0	−4.7	−1.9	−0.4	−36.4
	0.50	44.8	−71.9	−9.6	−6.2	−1.7	−44.6
	0.625	52.3	−63.3	−15.0	−12.9	−3.7	−42.6
	0.75	55.3	−38.5	−20.0	−21.5	−6.7	−31.4
	0.875	53.9	−1.9	−23.2	−32.0	−10.9	−14.1
	1.00	49.0	39.9	−23.7	−43.5	−16.5	5.2
0.78	0.001	11.7	0	0	0	0	11.7
	0.125	16.5	−13.2	−0.1	0	0	3.2
	0.25	28.1	−41.4	−1.5	−0.3	−0.1	−15.2
	0.375	41.4	−64.5	−5.2	−2.3	−0.6	−31.2
	0.50	52.2	−71.0	−10.5	−7.2	−1.9	−38.3
	0.625	58.8	−58.5	−16.0	−14.5	−4.2	−34.4
	0.75	60.4	−29.2	−20.8	−23.8	−7.6	−21.0
	0.875	57.5	11.4	−23.4	−35.0	−12.3	−1.9
	1.00	51.0	55.7	−22.8	−47.0	−18.6	18.3

The effective mass is then chosen to be

$$m^*=1.0 \tag{4.23}$$

for the particle spectrum, and

$$m_0^*=1.1,\ 1.5,\ 2.0,\ 2.5, \tag{4.24}$$

for the hole spectrum.

TABLE IV. Diagonal G_L-matrix elements (in Å), calculated on the energy shell. Statistical weights included. k_0 is varied. $\Delta=0.5$ and $m_0^*=1.5$.

k_F(Å^{-1})	k_0/k_F	$L=0$	$L=1$	$L=2$	$L=3$	$L>3$	Total
0.75	0.001	12.1	0	0	0	0	12.1
	0.125	16.3	−12.1	−0.1	0	0	4.1
	0.25	26.8	−38.9	−1.3	−0.3	0	−13.7
	0.375	38.9	−62.0	−4.7	−1.9	−0.4	−30.2
	0.50	48.9	−70.6	−9.6	−6.2	−1.7	−39.1
	0.625	55.0	−61.9	−15.0	−12.9	−3.7	−38.4
	0.75	56.6	−37.5	−19.9	−21.5	−6.7	−29.1
	0.875	53.8	−2.0	−23.2	−32.0	−10.9	−14.3
	1.00	47.6	37.9	−23.8	−43.6	−16.5	1.6
0.78	0.001	19.5	0	0	0	0	19.5
	0.125	24.0	−13.0	−0.1	0	0	10.9
	0.25	34.9	−40.8	−1.5	−0.3	−0.1	−7.8
	0.375	47.2	−63.4	−5.2	−2.3	−0.6	−24.3
	0.50	56.7	−69.4	−10.4	−7.2	−1.9	−32.3
	0.625	61.8	−56.9	−16.0	−14.5	−4.2	−29.7
	0.75	61.8	−28.0	−20.7	−23.8	−7.6	−18.3
	0.875	57.4	11.3	−23.4	−35.0	−12.3	−2.1
	1.00	49.6	53.4	−23.0	−47.1	−18.6	14.3

For the other parameters we have used

$$\Delta=0.4,\ 0.5,$$
$$k_0/k_F=0.001,\ 0.125,\ 0.25,\ 0.375,\ 0.50,\ 0.625,\ 0.75,\ 0.857,\ 1.00. \tag{4.25}$$

The parameter Δ is chosen such that γ^2 is always positive

TABLE V. Diagonal G-matrix elements (in Å), calculated on the energy shell. Δ and k_0 are varied. $m_0^*=2.5$.

k_0/k_F \ Δ	$k_F=0.75$ Å^{-1} 0.4	0.5	$k_F=0.78$ Å^{-1} 0.4	0.5
0.001	5.1	12.1	11.7	19.5
0.125	−2.9	4.2	3.2	11.0
0.25	−20.4	−13.1	−15.2	−7.1
0.375	−36.4	−28.7	−31.2	−22.7
0.50	−44.6	−36.4	−38.3	−29.3
0.625	−42.6	−33.9	−34.4	−24.7
0.75	−31.4	−22.0	−21.0	−10.6
0.875	−14.1	−4.0	−1.9	9.3
1.00	5.2	16.0	18.3	30.2

for a given m_0^*, i.e.,

$$\gamma^2=2\Delta k_F^2-k_0^2/m_0^*\geq k_F^2(2\Delta-1/m_0^*)>0 \quad \text{if} \quad \Delta>(2m_0^*)^{-1}. \tag{4.26}$$

A connection with Eq. (4.20) would be

$$\Delta=(2m_0^*)^{-1}-\mu/k_F^2, \tag{4.27}$$

TABLE VI. Diagonal G-matrix elements (in Å), calculated on the energy shell. m_0^* and k_0 are varied. $\Delta=0.5$.

k_0/k_F \ m_0^*	$k_F=0.75$ Å^{-1}				$k_F=0.78$ Å^{-1}			
	1.1	1.5	2.0	2.5	1.1	1.5	2.0	2.5
0.001	12.1	12.1	12.1	12.1	19.5	19.5	19.5	19.5
0.125	3.9	4.1	4.2	4.2	10.7	10.9	11.0	11.0
0.25	−14.2	−13.7	−13.3	−13.1	−8.4	−7.8	− 7.4	−7.1
0.375	−31.5	−30.2	−29.3	−28.7	−25.8	−24.3	−23.3	−22.7
0.50	−41.6	−39.1	−37.4	−36.4	−35.0	−32.3	−30.4	−29.3
0.625	−42.6	−38.4	−35.6	−33.9	−34.4	−29.7	−26.6	−24.7
0.75	−35.6	−29.1	−24.6	−22.0	−25.5	−18.3	−13.5	−10.6
0.875	−23.9	−14.3	−7.9	−4.0	−12.7	−2.1	5.1	9.3
1.00	−12.2	1.6	10.6	16.0	−0.8	14.3	24.3	30.2

as can be seen from Eqs. (3.15) and (3.20). The average momentum P is always set equal to zero.

If the constant A in Eqs. (3.14) or (3.15) is chosen equal to zero for the single-particle energy spectrum for intermediate states, the values for Δ in Eq. (4.25) correspond to the following values for the constant A_0 which defines the input hole spectrum,

$$\begin{aligned} A_0 &= -3.7, -4.6\text{°K} \quad \text{for} \quad k_0=0.75\ \text{Å}^{-1}, \\ &= -4.0, -5.0\text{°K} \quad \text{for} \quad k_0=0.78\ \text{Å}^{-1}, \end{aligned} \tag{4.28}$$

as can be seen from Eq. (3.20).

To estimate the importance of including the exclusion principle, we have also calculated the main first-order term in the original reference spectrum method of Bethe *et al.*,[5] using the same energy spectrum as in the BG method. That is, we have neglected the exclusion principle and used Eq. (3.38) instead of Eq. (3.36) for the Green's functions $\Gamma_L(r,r')$ when solving the Bethe-Goldstone equation (3.34). The results from the two methods are compared in Table I for the S wave, and for some typical standard parameter values.

For partial waves with $L>3$, we have replaced the perturbed wave function $u_L(k_0,r)$ in Eq. (3.31) by the unperturbed one $\mathcal{J}_L(k_0r)$, i.e., we have made the approximation

$$\int_0^\infty \mathcal{J}_L(k_0r)v(r)u_L(k_0,r)dr \approx \int_0^\infty \mathcal{J}_L{}^2(k_0r)v(r)dr. \tag{4.29}$$

Then it is not necessary to solve the Bethe-Goldstone equation first to get the true wave function $u_L(k_0,r)$, and we calculate Eq. (3.31) as

$$\sum_L \langle k_0|V_L|k_0\rangle = (4\pi/k_0^2)\Big[\sum_{\text{even } L} + 3\sum_{\text{odd } L}\Big](2L+1) \times \int_0^\infty \mathcal{J}_L{}^2(k_0r)v(r)dr. \tag{4.30}$$

Some calculations to check this approximation are shown in Table II. The mesh chosen for the radial integration with this approximation is

$$r=2.4(0.1)20.0\ \text{Å}. \tag{4.31}$$

TABLE VII. Nondiagonal G-matrix elements $\langle k|G_L|k_0\rangle$ (in Å), calculated on the energy shell for $L<4$. Statistical weights included. k is varied. $\Delta=0.4$, $m_0^*=2.0$, and $k_0=0.5k_F$.

k_F(Å^{-1})	k/k_F	$L=0$	$L=1$	$L=2$	$L=3$	Total
0.75	0.001	30.6	0	0	0	30.6
	0.1	31.2	−22.8	−0.6	−0.1	7.7
	0.2	33.0	−43.2	−2.3	−0.7	−13.1
	0.3	35.9	−59.0	−4.7	−2.0	−29.7
	0.4	39.7	−68.9	−7.3	−4.0	−40.4
	0.5	44.1	−72.2	−9.6	−6.2	−44.0
	0.6	48.7	−68.9	−11.5	−8.3	−40.0
	0.7	53.1	−59.7	−12.6	−9.8	−29.0
	0.8	57.1	−45.9	−12.9	−10.7	−12.4
	0.9	60.3	−28.6	−12.7	−10.9	8.1
	1.0	62.3	−9.3	−11.9	−10.7	30.4
0.78	0.001	38.3	0	0	0	38.3
	0.1	38.9	−23.3	−0.7	−0.1	14.8
	0.2	40.7	−44.0	−2.5	−0.8	−6.7
	0.3	43.5	−59.8	−5.1	−2.3	−23.8
	0.4	47.2	−69.1	−7.9	−4.6	−34.5
	0.5	51.4	−71.3	−10.5	−7.2	−37.5
	0.6	55.7	−66.5	−12.3	−9.4	−32.5
	0.7	59.9	−55.5	−13.4	−11.0	−19.9
	0.8	63.4	−39.6	−13.6	−11.8	−1.6
	0.9	65.9	−20.4	−13.2	−11.9	20.4
	1.0	67.3	0.7	−12.2	−11.7	44.1

TABLE VIII. Nondiagonal G-matrix elements $\langle k|G_L|k_0\rangle$ (in Å), calculated on the energy shell for $L<4$. Statistical weights included. k is varied. $\Delta=0.4$, $m_0^*=2.0$, and $k_0=k_F$.

k_F(Å^{-1})	k/k_F	$L=0$	$L=1$	$L=2$	$L=3$	Total
0.75	0.001	52.9	0	0	0	52.9
	0.1	52.9	−6.0	−0.6	−0.1	46.2
	0.2	52.7	−11.2	−2.3	−0.8	38.4
	0.3	52.5	−15.1	−4.9	−2.6	29.8
	0.4	52.1	−16.8	−8.4	−5.9	21.0
	0.5	51.6	−16.0	−12.2	−10.8	12.7
	0.6	51.0	−12.0	−16.0	−17.0	5.9
	0.7	50.2	−4.7	−19.5	−24.2	1.8
	0.8	49.3	6.1	−22.2	−31.5	1.7
	0.9	48.2	20.1	−23.7	−38.2	6.4
	1.0	46.9	36.9	−23.9	−43.7	16.2
0.78	0.001	58.1	0	0	0	58.1
	0.1	58.0	−4.2	−0.6	−0.1	53.1
	0.2	57.7	−7.6	−2.3	−0.9	46.9
	0.3	57.3	−9.6	−5.1	−2.8	39.8
	0.4	56.6	−9.6	−8.6	−6.4	32.1
	0.5	55.8	−7.0	−12.4	−11.8	24.6
	0.6	54.8	−1.4	−16.3	−18.6	18.5
	0.7	53.6	7.4	−19.7	−26.4	14.9
	0.8	52.2	19.4	−22.1	−34.4	15.2
	0.9	50.6	34.6	−23.3	−41.6	20.3
	1.0	48.8	52.2	−23.1	−47.2	30.8

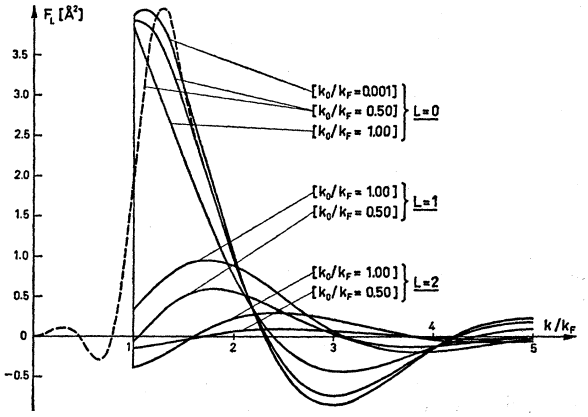

FIG. 10. Fourier transforms $F_L(k)$ of $\chi_L(k_0,r)/k_0$, defined by Eq. (3.24). Dotted line is $F_0(k)$ calculated according to Eq. (3.21). k_0 is varied. $k_F=0.75$ Å^{-1}, $\Delta=0.4$, and $m_0^*=2.0$.

The mesh chosen for all the other integrations is

$$r,r'=0.3(0.2)0.7(0.1)3.0(0.2)5.0(0.5)10.0(1.0)12.0 \text{ Å}. \quad (4.32)$$

The integration is carried out to a distance such that contributions beyond this distance can be assumed to be negligible.

The mesh used for the numerical integration in momentum space, when calculating κ or Eq. (3.27), is

$$k/k_F=1.0(0.1)5.0. \quad (4.33)$$

In the numerical integration of Eq. (3.37) for $\Gamma_L(r,r')$, a mesh

$$k/k_F=0(0.05)1.0 \quad (4.34)$$

is found to be sufficient.

Results from the two-body calculations are then shown in Tables I–XIV and in Figs. 3–15.

Tables I–IX give G-matrix elements in dimension Å, which can be converted to °K Å^3 according to Eq. (3.28). Table X gives the binding energy, with only two-body terms included, in dimension °K. Tables XI and XII give the volume integral of the square of the defect wave function, i.e., the convergence parameter κ_L defined by Eqs. (3.26) or (3.27), in dimension Å^3. The total κ, i.e., the expression (3.25) or (3.26), is shown in Tables XIII and XIV. It is just the sum of the terms in Tables XI and XII multiplied by the factor $\pi\rho$ to get the dimensionless and density-independent expression for κ.

5. SUMMARY AND DISCUSSION

From the various tables and diagrams we can see how the results change as the input parameters are varied. The only fixed parameter in our calculations is the effective mass $m^*=1$ for the particle energy spectrum off the energy shell. It should be a fairly good approximation to choose the intermediate-state potentials to be essentially zero as we have done, i.e., put $m^*=1$. But then it is necessary to make a separate calculation of the three-body cluster energy as we are

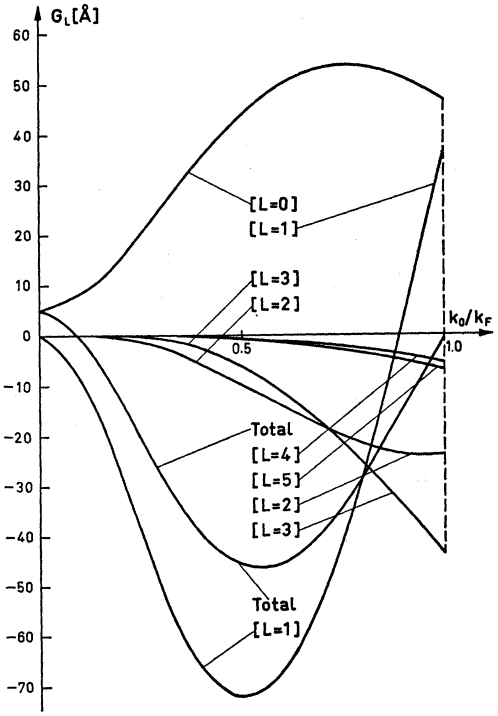

FIG. 11. Diagonal G-matrix elements $\langle k_0|G_L|k_0\rangle$, calculated on the energy shell. $k_F=0.75$ Å^{-1}, $\Delta=0.4$, and $m_0^*=2.0$.

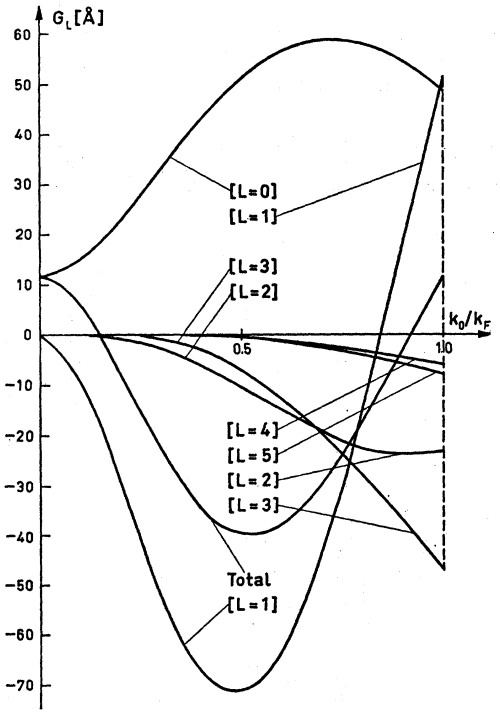

FIG. 12. Diagonal G-matrix elements $\langle k_0|G_L|k_0\rangle$, calculated on the energy shell. $k_F=0.78$ Å^{-1}, $\Delta=0.4$, and $m_0^*=2.0$.

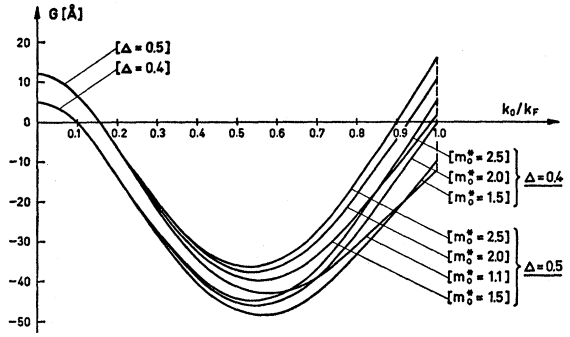

FIG. 13. Diagonal G-matrix elements $\langle k_0|G|k_0\rangle$, calculated on the energy shell. m_0^* is varied. $k_F=0.75$ Å^{-1}.

going to do in a forthcoming paper. Also, the average momentum P or the c.m. momentum $2P$ is set equal to zero. Inclusion of P has been shown not to be important in nuclear-matter calculations for central forces only,[16] and it should be a fair approximation to neglect it. The other parameters have been varied to cover their probable values.

The variation of the G-matrix elements, the binding energy, and the convergence parameter κ can be seen in the tables. The diagrams show the variation or behavior of the two-body wave functions, the effective interactions, the Fourier transforms of $\chi_L(k_0,r)$, and the G-matrix elements. In solving the Bethe-Goldstone equation to get the wave functions, we had to use matrix inversion in our calculations, because an iteration procedure would not converge. This problem of convergence is due to the strongly repulsive soft core in the potential.

Outside of about 3 Å, the effective interaction $g_L(r)$ has an exponential behavior very similar to the two-body potential $v(r)$, and they are equal for large distances. It seems, however, rather difficult to find some simple analytic function which could replace $g_L(r)$ approximately. It is a complicated problem to calculate $g_L(r)$ accurately because of the unpleasant zeros in the wave function $\mathcal{J}_L(k_0r)$. In our calculations we have just used some averaging and interpolation method to correct $g_L(r)$ at each such point, taking into account the value of $v(r)$ at that point. But it would be nice to have a more exact method, especially because a calculation of the three-body energy term would be very sensitive to the effective interaction $g_L(r)$ off the energy shell.

The Fourier transforms can be calculated in two different ways, according to Eqs. (3.21) or (3.24), as stated in Sec. 3. Here it seems more accurate to work with the true wave function $u_L(k_0,r)$ in Eq. (3.24) than with the distortion $\chi_L(k_0,r)$ in Eq. (3.21). This is because the values for $\chi_L(k_0,r)$ will be more uncertain and have a greater relative error than the values for the wave function $u_L(k_0,r)$. Also, the exclusion operator $Q(P,k)$

[16] G. Dahll, E. Østgaard, and B. Brandow, Nucl. Phys. (to be published).

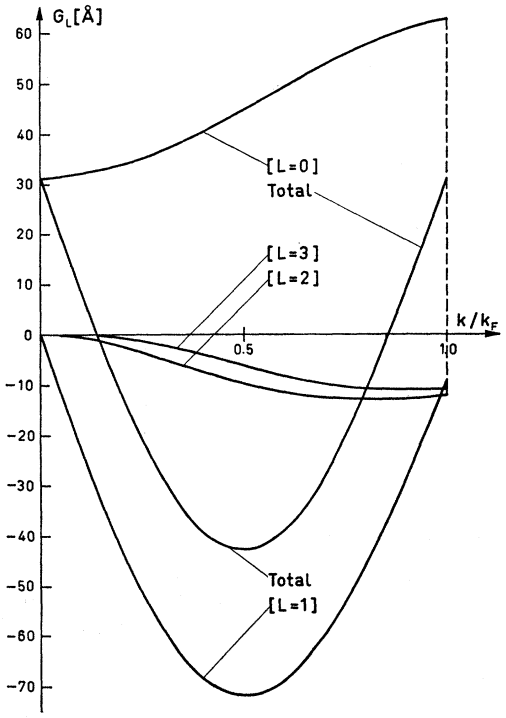

FIG. 14. Nondiagonal G-matrix elements $\langle k|G_L|k_0\rangle$, calculated on the energy shell. The total G matrix is with only $L<4$ included. $k_F=0.75$ Å^{-1}, $\Delta=0.4$, $m_0^*=2.5$, and $k_0=0.5k_F$.

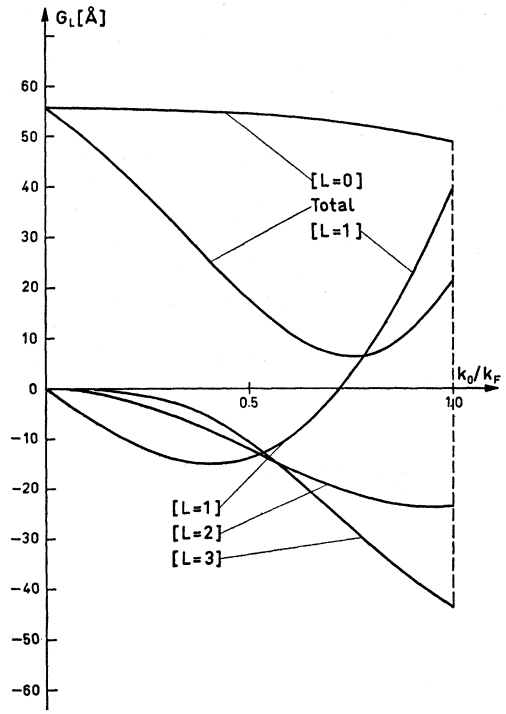

FIG. 15. Nondiagonal G-matrix elements $\langle k|G_L|k_0\rangle$, calculated on the energy shell. The total G matrix is with only $L<4$ included. $k_F=0.75$ Å^{-1}, $\Delta=0.4$, $m_0^*=2.5$, and $k_0=k_F$.

TABLE IX. Diagonal G_L-matrix elements (in Å) for $L>3$, calculated as $\langle k_0|V_L|k_0\rangle$ defined by Eq. (4.30). Statistical weights included. k_0 is varied.

k_F(Å^{-1})	k_0/k_F	$L=4$	$L=5$	$L=6$	$L=7$	$L=8$	$L=9$	$L=10$	$L=11$	Total
0.75	0.125	0	0	0	0	0	0	0	0	0
	0.25	−0.03	−0.01	0	0	0	0	0	0	−0.04
	0.375	−0.25	−0.18	−0.01	0	0	0	0	0	−0.44
	0.50	−0.69	−0.78	−0.10	−0.08	−0.01	0	0	0	−1.65
	0.625	−1.35	−1.63	−0.26	−0.37	−0.05	−0.01	0	0	−3.66
	0.75	−2.35	−2.86	−0.45	−0.73	−0.14	−0.20	0	0	−6.73
	0.875	−3.73	−4.58	−0.74	−1.18	−0.23	−0.43	−0.05	0	−10.93
	1.00	−5.50	−6.88	−1.10	−1.80	−0.35	−0.65	−0.13	−0.10	−16.51
0.78	0.125	0	0	0	0	0	0	0	0	0
	0.25	−0.04	−0.01	0	0	0	0	0	0	−0.05
	0.375	−0.29	−0.23	−0.02	−0.01	0	0	0	0	−0.55
	0.50	−0.77	−0.90	−0.12	−0.12	−0.01	0	0	0	−1.92
	0.625	−1.53	−1.83	−0.29	−0.44	−0.07	−0.05	0	0	−4.21
	0.75	−2.65	−3.23	−0.51	−0.82	−0.16	−0.26	0	0	−7.63
	0.875	−4.18	−5.16	−0.83	−1.34	−0.26	−0.48	−0.05	−0.01	−12.31
	1.00	−6.15	−7.75	−1.25	−2.02	−0.40	−0.73	−0.14	−0.11	−18.55

in Eq. (3.24) gives a more correct behavior at $k\approx k_F$. When using the transformation $(Q/e)vu_L$, i.e., Eq. (3.22) in Eq. (3.24), the explicit appearance of Q ensures the correct behavior near k_F, while the presence of $v(r)$ gives a satisfactory convergence of the integration in coordinate space.

In the calculations of the binding energy, we see that the repulsion for $L=0$ and the attraction for $L=1$ roughly cancel each other. The partial waves with $L>1$ thus give us the binding. The binding energy of liquid ^{3}He is calculated for several values of the input parameters. The results are given in Table X, and can be compared with values from other calculations: −0.20°K/particle of Massey and Woo,[17] −0.96°K of BG,[1] −1.16°K of Beck and Sessler,[18] and −1.35°K of Schiff and Verlet,[19] while the experimental value is −2.5°K/particle.[7,8]

A special point in our calculations is the problem of the energy denominator in the Bethe-Goldstone equation. Here it is very useful to have a reference spectrum or an effective-mass approximation. The release of the energy denominator from the loop of self-consistency through the G-matrix elements and the single-particle potentials is a great advantage in the calculations, and here we should try to use the idea of a reference energy spectrum if possible.

TABLE X. Binding energy for liquid ^{3}He (in °K). Only two-body terms included. Δ and m_0^* are varied.

k_F(Å^{-1})	Δ \ m_0^*	1.1	1.5	2.0	2.5
0.75	0.4		−1.69	−1.43	−1.27
	0.5	−1.08	−0.71	−0.45	−0.29
0.78	0.4		−1.12	−0.79	−0.59
	0.5	−0.36	0.11	0.43	0.61

[17] W. E. Massey and C. W. Woo, Phys. Rev. **164**, 256 (1967).
[18] D. E. Beck and A. M. Sessler, Phys. Rev. **146**, 161 (1966).
[19] D. Schiff and L. Verlet, Phys. Rev. **160**, 208 (1967).

In liquid ^{3}He the "true" effective mass has a large value which means a flattening of the energy spectrum with respect to that of free particles. This is because of an increase in the depth of the single-particle potential as the Fermi surface is approached, which partially compensates the increase in the kinetic energy, giving the large effective mass. For slow particles near the bottom of the Fermi distribution, the repulsive core acts strongly and the repulsion is enhanced by the exclusion principle. For more rapidly moving particles near the Fermi surface, the interaction in states of higher angular momentum becomes more effective. The repulsive effect decreases, the attractive interaction increases, and the interaction energy becomes more negative as the Fermi surface is approached. The potential energy of interaction thus increases as the particle momentum increases, giving the large effective mass.

If we choose the intermediate-state single-particle potentials equal to zero, and require that a binding

TABLE XI. Volume integrals κ_L of the correlation hole (in Å^3), defined by Eq. (3.26). Calculated on the energy shell for $L<4$. Statistical weights included. k_0 is varied. $\Delta=0.4$ and $m_0^*=2.5$.

k_F(Å^{-1})	k_0/k_F	$L=0$	$L=1$	$L=2$	$L=3$	Total
0.75	0.001	5.01	0	0	0	5.01
	0.125	4.96	0.10	0	0	5.06
	0.25	4.84	0.39	0	0	5.23
	0.375	4.63	0.85	0.01	0	5.49
	0.50	4.35	1.44	0.03	0.01	5.83
	0.625	4.01	2.12	0.07	0.02	6.22
	0.75	3.65	2.84	0.12	0.05	6.66
	0.875	3.25	3.57	0.20	0.10	7.12
	1.00	2.84	4.29	0.28	0.19	7.60
0.78	0.001	5.09	0	0	0	5.09
	0.125	5.04	0.11	0	0	5.15
	0.25	4.90	0.42	0	0	5.32
	0.375	4.67	0.91	0.01	0	5.59
	0.50	4.37	1.53	0.03	0.01	5.94
	0.625	4.00	2.25	0.07	0.02	6.34
	0.75	3.60	3.01	0.13	0.05	6.79
	0.875	3.18	3.77	0.20	0.11	7.26
	1.00	2.74	4.51	0.29	0.20	7.74

energy calculated from our input hole spectrum be equal to the binding energy given by the output G-matrix elements, we get self-consistent solutions of approximately -0.5°K/particle for $k_F=0.75$ Å^{-1} and -0.3°K/particle for $k_F=0.78$ Å^{-1}. This is, however, only an indication. We have probably lost some binding energy by putting the c.m. momentum equal to zero. This also has some effect on the slope of our output single-particle spectrum, and there is not much point in trying to obtain, for instance, a self-consistent effective mass from our results. Our assumption of rather different particle and hole spectra near the Fermi momentum k_F is another reason for not calculating a true effective mass.

We have simplified the original BG method and made it more convenient in two ways. The first is to express the total Green's function $\Gamma_L(r,r')$ as the reference spectrum Green's function (3.38), which has an analytic form, plus a correction term which takes the exclusion principle into account, and in which the range of integration in momentum space is only of order k_F. The second way is to use the reference spectrum idea of Bethe for the energy denominator in the Bethe-Goldstone equation, as already mentioned. But the use of single-particle energies calculated from G-matrix elements, in the energy denominator, is an important feature of the original BG calculations, and could possibly be an improvement in our calculations. This would, however, involve extensive computational time.

It would be nice if one could simplify the BG method further, but this is probably not possible. For nuclear-matter calculations, Moszkowski and Scott[20] simplified the problem by separating the potential into a short-range and a long-range part. The separation distance should be chosen in such a way that the short-range part alone gives zero phase shift for ordinary free-particle scattering. The idea is to eliminate the repulsion and a compensating part of the attraction, and work only with the remaining interaction outside the separation distance. But it is obviously not possible to use this method in calculations for liquid ^{3}He, where the S wave and also partly the P wave give a net repulsion.

It is not possible, either, to neglect the Pauli principle, i.e., to put the exclusion operator $Q=1$, as in the reference-spectrum method of Bethe *et al.*[5] From Table I it is obvious that the exclusion principle cannot be neglected as a first approximation, and it seems that of the three important methods used in nuclear-matter calculations, only the BG method can be used in calculations for liquid ^{3}He.

The forces which are used in the calculations are derived from experiments on the energy shell, while in the calculations we are sometimes probably rather far off the energy shell. The extrapolation is made by assuming that the forces are still given by a potential, but this may not be quite correct.

The chosen potential seems to have a very strong influence on the results of the calculations. Potentials with different shapes will generally give different results or predictions, and the value obtained for the binding energy is extremely sensitive to changes in the various parts of the potential. This is because the binding energy is actually a small difference between large repulsive and attractive terms. The repulsion comes from the large repulsive region in the potential and the high zero-point Fermi energy, and is only slightly overcompensated by the attractive part of the potential. Also, the repulsive soft core in the potential is not well

TABLE XII. Volume integrals κ_L of the correlation hole (in Å^3), defined by Eq. (3.26). Calculated on the energy shell for $L<4$. Statistical weights included. k_0 is varied. $\Delta=0.5$ and $m_0^*=1.5$.

k_F(Å^{-1})	k_0/k_F	$L=0$	$L=1$	$L=2$	$L=3$	Total
0.75	0.001	4.87	0	0	0	4.87
	0.125	4.83	0.10	0	0	4.93
	0.25	4.72	0.38	0	0	5.10
	0.375	4.52	0.84	0.01	0	5.37
	0.50	4.27	1.42	0.03	0	5.72
	0.625	3.96	2.10	0.06	0.02	6.14
	0.75	3.61	2.83	0.12	0.05	6.61
	0.875	3.25	3.58	0.20	0.10	7.13
	1.00	2.88	4.32	0.29	0.20	7.69
0.78	0.001	4.95	0	0	0	4.95
	0.125	4.91	0.10	0	0	5.01
	0.25	4.77	0.41	0	0	5.18
	0.375	4.56	0.89	0.01	0	5.46
	0.50	4.28	1.51	0.03	0.01	5.83
	0.625	3.94	2.23	0.07	0.02	6.26
	0.75	3.57	3.00	0.12	0.05	6.74
	0.875	3.18	3.77	0.20	0.11	7.26
	1.00	2.77	4.54	0.30	0.21	7.82

[20] S. A. Moszkowski and B. L. Scott, Ann. Phys. (N. Y.) **11**, 65 (1960).

TABLE XIII. Convergence parameter κ calculated on the energy shell. Δ and k_0 are varied. $m_0^*=2.5$.

k_0/k_F \ Δ	$k_F=0.75$ Å^{-1} 0.4	0.5	$k_F=0.78$ Å^{-1} 0.4	0.5
0.001	0.223	0.217	0.256	0.249
0.125	0.226	0.220	0.259	0.252
0.25	0.233	0.227	0.267	0.260
0.375	0.245	0.239	0.281	0.274
0.50	0.260	0.253	0.298	0.290
0.625	0.278	0.270	0.319	0.310
0.75	0.296	0.289	0.341	0.332
0.875	0.317	0.309	0.364	0.355
1.00	0.339	0.329	0.389	0.378

TABLE XIV. Convergence parameter κ calculated on the energy shell. m_0^* and k_0 are varied. $\Delta=0.5$.

k_0/k_F \ m_0^*	$k_F=0.75$ Å^{-1} 1.1	1.5	2.0	2.5	$k_F=0.78$ Å^{-1} 1.1	1.5	2.0	2.5
0.001	0.217	0.217	0.217	0.217	0.249	0.249	0.249	0.249
0.125	0.220	0.220	0.220	0.220	0.252	0.252	0.252	0.252
0.25	0.228	0.227	0.227	0.227	0.261	0.261	0.260	0.260
0.375	0.241	0.240	0.239	0.239	0.276	0.275	0.274	0.274
0.50	0.257	0.255	0.254	0.253	0.295	0.293	0.291	0.290
0.625	0.278	0.274	0.272	0.270	0.319	0.314	0.312	0.310
0.75	0.300	0.295	0.291	0.289	0.346	0.339	0.334	0.332
0.875	0.326	0.317	0.312	0.309	0.375	0.365	0.358	0.355
1.00	0.357	0.342	0.334	0.329	0.410	0.393	0.383	0.378

known, and may give relatively large errors in the calculations.

We have not worried about this problem in our work, but have concentrated upon other parameters. If we could trust the BG method, we could say something about the potentials. If we could trust a potential, we could tell more about the BG method. At the moment, it seems that we neither know the correct potential nor are we sure about the method. But some qualitative results and conclusions should be generally valid, independent of the specific potential which is used in the calculations.

The main conclusion is that our calculations give approximately the same results for the two-body potential energy and the single-particle energy spectrum as the calculations of Brueckner and Gammel[1] and others.[17–19] The binding energy with only two-body terms included is approximately -1°K/particle or more likely only $-\frac{1}{2}$°K/particle. In a future paper we shall see if we can get some additional binding energy from three-body correlations.

ACKNOWLEDGMENTS

The author would like to thank Professor G. E. Brown for helpful suggestions and stimulating discussions. He is also grateful for the support and kind hospitality of NORDITA in Copenhagen, where this work was begun.

PHYSICAL REVIEW VOLUME 170, NUMBER 1 5 JUNE 1968

Positive-Ion Mobilities in Dry Air*

G. SINNOTT, D. E. GOLDEN, AND R. N. VARNEY
Lockheed Palo Alto Research Laboratory, Palo Alto, California
(Received 15 January 1968)

Drift velocities of mass-identified positive ions in air have been measured to about $\pm 5\%$ as a function of E/N for $2\times10^{-16}\lesssim E/N\lesssim 2\times10^{-14}$ V cm^2 and for $1.8\times10^{15}\lesssim N\lesssim 7\times10^{15}$ cm^{-3}. These measurements lead to values of the zero-field mobilities of 1.6, 3.5, and 2.5 cm^2/V sec for N_2^+, NO^+, and O_2^+, respectively, in air. The high-E/N data yield momentum-transfer cross sections of 110, 21, and 30 Å^2 for N_2^+, NO^+, and O_2^+, respectively. The rapid disappearance of N^+ and O^+ due to ion-molecule reactions prevented good drift-velocity measurements for them, but partial results indicate that O^+ is about 5% faster, and N^+ about 10% faster, than NO^+ in air. N_2^+ is shown to disappear rapidly by charge transfer with O_2. Thus, although the classical value of 1.6 is obtained for the mobility of N_2^+ in air, N_2^+ cannot be present long enough at pressures close to atmospheric to account for the classical observations.

I. INTRODUCTION

THIS paper reports measurements of the drift velocities and hence the mobilities of mass-identified positive ions in air. It results from an investigation of both the ion-molecule reactions and drift velocities of ions in dry air carried out in a drift tube. Details of the reactions studied will be presented elsewhere.[1]

Among the several methods of measuring the mobilities of ions in gases, the double-shutter, drift-velocity spectrometer of Tyndall, Starr, and Powell[2] operated with square-wave voltage is the most direct and versatile. The device can be connected in tandem with a mass spectrometer to provide both mass analysis and drift-velocity analysis of the same ions. The resulting data can be easily interpreted even in the presence of complicated ion-molecule reactions; in fact, the same apparatus can be used to measure many ion-molecule reaction rates. The ability to make meaningful measurements on complicated gas-ion systems accounts for the increase in popularity of the method in recent years.[3]

The present work has been carried out in dry air at pressures below 0.2 Torr. The findings are thus pertinent to the ionosphere, where the altitude and the temperature combine to produce similar or lower pressures and low humidity. The disagreements with the older measurements on positive ions in air, while failing to identify the ions studied by Bradbury[4] and others, do eliminate some surmises concerning the ions in the older experiments.

* Work supported by Lockheed Independent Research Funds.
[1] D. E. Golden and G. Sinnott (unpublished).
[2] A. M. Tyndall, L. H. Starr, and C. F. Powell, Proc. Roy. Soc. (London) 121, 172 (1928).
[3] For some other apparatus incorporating tandem drift-velocity mass analysis, see E. W. McDaniel, D. W. Martin, and W. S. Barnes, Rev. Sci. Instr. 33, 2 (1962); K. B. McAfee and D. Edelson, in *Proceedings of the Sixth International Conference on Ionization Phenomena in Gases, Paris, 1963* (SERMA, Paris, 1964), Vol. I, p. 299; M. Saporoschenko, Phys. Rev. 139, A349 (1965); Y. Kaneko, L. R. Megill, and J. B. Hasted, J. Chem. Phys. 45, 3741 (1966); P. Warneck, *ibid.* 46, 502 (1967); J. Heimerl, R. Johnsen, and M. A. Biondi, Abstracts of the Twentieth Annual Gaseous Electronics Conference, San Francisco, 1967 (unpublished).
[4] N. E. Bradbury, Phys. Rev. 40, 508 (1932).